

Parallels Between Quantum Antiferromagnetism and the Strong Interactions

R. B. Laughlin*

Department of Physics, Stanford University, Stanford, CA 94305

(Dated: October 1, 1997)

I suggest that the great body of knowledge gained over the past 10 years about simple spin-1/2 quantum quantum antiferromagnets points to a connection between cuprate superconductivity and the strong interactions. The underlying physical idea is that the phase diagram of such a magnet consists of competing ordered phases regulated by a nearby quantum critical point. Exactly at this critical point the low-lying elementary excitations of the magnet are gauge fields and particles with fractional quantum numbers analogous to the spinon and holon excitations found in spin chains. An arbitrarily small distance away, however, these bind at low energy scales to make the familiar collective modes of the ordered states into which one renormalizes. Vestiges of these “parts” of the collective modes may be seen in conventional materials and models in high-energy spectroscopy and inconsistencies in sum rules exactly the way quarks are seen in particle physics. [Published in Proc. of the Inaugural Conf. of the APCTP, ed. by Y. M. Cho, J.B. Hong, and C. N. Yang (World Sci., Singapore, 1998).]

PACS numbers: 71.27.+a, 74.20.+a, 74.20.-z, 11.15.Ha

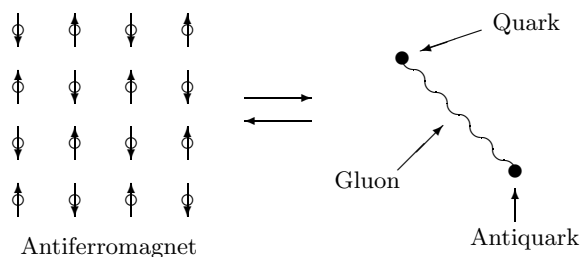


FIG. 1: The physical behavior of the strong interactions generated spontaneously in simple antiferromagnets.

The premise of this article is illustrated in Fig. 1. I wish to argue that there are physically identifiable objects in simple Heisenberg antiferromagnets which behave like U(1) quarks and could conceivably be apt analogues of them. These are not the elementary excitations of the system in most cases but rather objects out of which the elementary excitations are built. It is my current belief that the quark-like objects and the gauge fields through which they interact are the true elementary excitations at some nearby quantum critical point, but I shall mostly sidestep this issue and concentrate on the physical meaningfulness of the particles in the commonly-studied cases.

The antiferromagnets in question are described by the t-J Hamiltonian

$$\mathcal{H} = P_G \mathcal{H}_o P_G \quad , \quad (1)$$

where

$$P_G = \prod_j \left\{ 1 - c_{j\uparrow}^\dagger c_{j\downarrow}^\dagger c_{j\downarrow} c_{j\uparrow} \right\} \quad (2)$$

is the Gutzwiller projector and

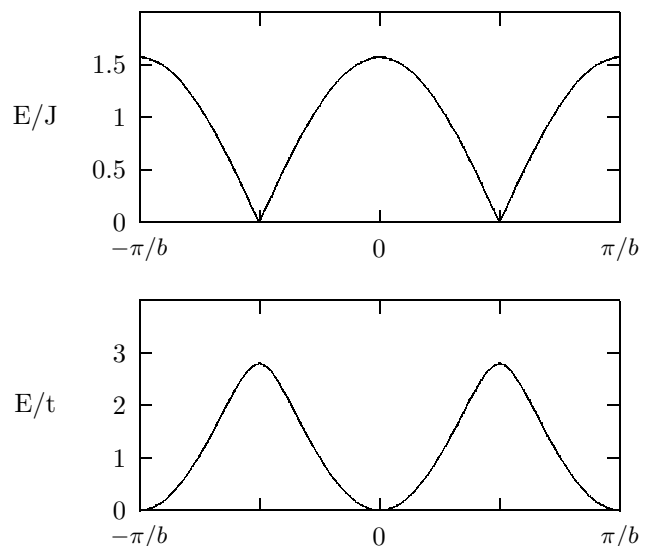


FIG. 2: Spinon (top) and holon (bottom) dispersion relations obtained by Bares, Blatter, and Ogata¹ from the Bethe ansatz solution of the supersymmetric spin chain.

$$\mathcal{H}_o = \sum_{\langle j,k \rangle} \left\{ -t \sum_{\sigma} c_{j\sigma}^\dagger c_{k\sigma} + \frac{J}{2} \mathbf{S}_j \cdot \mathbf{S}_k \right\} \quad , \quad (3)$$

the sum $\langle j,k \rangle$ being over near-neighbor pairs of a lattice, with each pair counted twice to maintain hermiticity. When the dimension of the lattice is 2 or greater, the phase diagram of this model is complex and beyond our means to compute reliably. When the dimension of the lattice is 1, however, there is an exact solution at the supersymmetric point $J = 2t$, the ground state of which is a nondegenerate singlet, i.e. has no order, and the elementary excitations of which are spin-1/2, charge-0

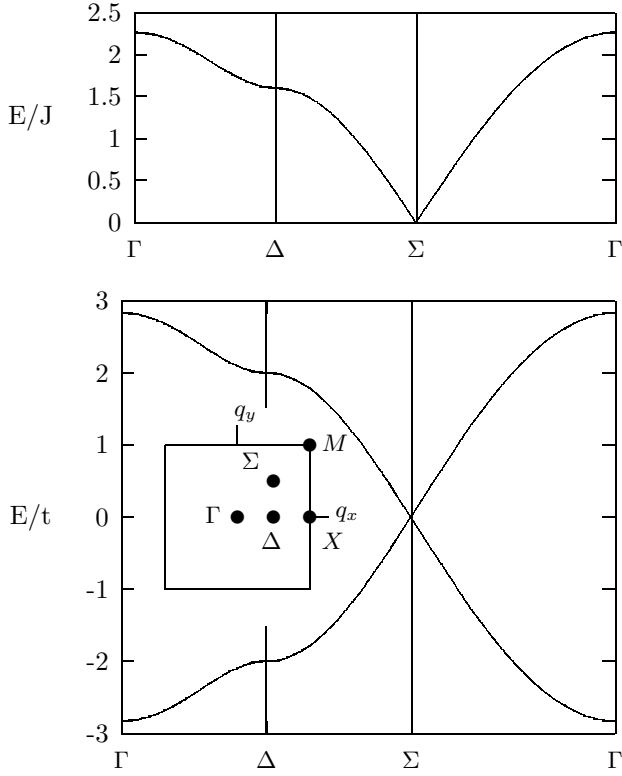


FIG. 3: 2-d spinon (top) and holon (bottom) dispersion relations given by Eqs. (4) and (5). The inset labels the special points in the Brillouin zone.

particles known as “spinons” and spin-0, charge-1 particles known as “holons”. These are the quark-like objects of the problem. Their dispersion relations are plotted in Fig. 2¹. The existence of spinons and holons is intimately connected with the lack of order in the ground state, and is thus common in 1 dimension, where continuous symmetry breaking is impossible, but uncommon in higher dimension, where order seems to occur almost always. But if the higher-dimensional ground state is *forced* to be disordered by means of a variational ansatz, which is equivalent to adding a small long-range interaction to the Hamiltonian to destabilize the order, then spinons and holons makes sense and we obtain in 2-d the dispersion relations²

$$E_q^{spinon} = 1.6J\sqrt{\cos^2(q_x) + \cos^2(q_y)} \quad (4)$$

$$E_q^{holon} = \pm 2t\sqrt{\cos^2(q_x) + \cos^2(q_y)} \quad (5)$$

plotted in Fig. 2. These are also implicit in the U(1) gauge theory descriptions of the t-J model based on the commensurate flux saddle point^{3,4}. I wish now to establish that these particles have physical meaning at intermediate energy scales even when the system is allowed

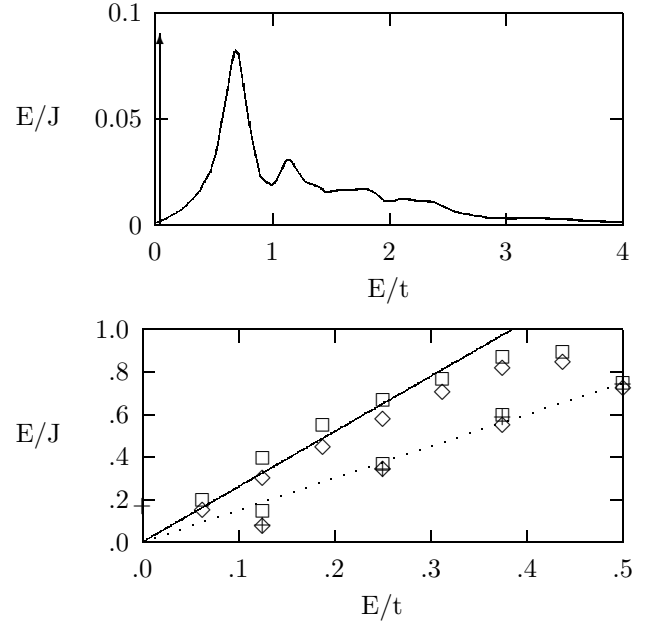


FIG. 4: Top: Optical conductivity computed by exact diagonalization by Moreo and Dagotto⁵ on a 4×4 cluster for the case of $\delta = 1/16$ and $J/t = 0.4$. The arrow at $\omega = 0$ indicates the Drude oscillator. Bottom: Total oscillator strength $-\langle T \rangle / Nt$ defined by Eq. (9) and its Drude contribution computed by exact diagonalization on a 4×4 cluster. The symbols \square , $+$, and \diamond correspond to $J/t = 0.1, 0.4$, and 1.0 , respectively. The solid curve is a plot of Eq. (11). The dotted curve is a guide to the eye.

to order, giving rise to forces that bind them at low energy scales into the well-known excitations of the ordered phases.

In Fig. 4 I show the optical conductivity

$$\sigma_{xx}(\omega) = \frac{1}{N} \frac{\pi}{\omega} \sum_{\alpha} |\langle \alpha | j_x | 0 \rangle|^2 \delta(\hbar\omega - E_{\alpha} + E_0) \quad (6)$$

computed by Dagotto and Moreo⁵ for a single hole in a 4×4 cluster, which is representative of such calculations. Here $|\alpha\rangle$ indicates an exact eigenstate of energy E_{α} and j_x is the electric current operator

$$j_x = P_G i \frac{t}{\hbar} \sum_j \sum_{\sigma} \left\{ c_{j\sigma}^{\dagger} c_{k\sigma} - c_{k\sigma}^{\dagger} c_{j\sigma} \right\} P_G \quad , \quad (7)$$

where k denotes the near neighbor of j in the x -direction. This calculation provides evidence for the existence of the holon and measures the size of its mass. The f -sum rule

$$\int_0^{\infty} \sigma_{xx}(\omega) d\omega = -\frac{\pi}{4} \frac{\langle 0 | T | 0 \rangle}{N} \quad (8)$$

is plotted versus doping in the lower part of the figure, as is its “Drude” contribution. The width and shape of the

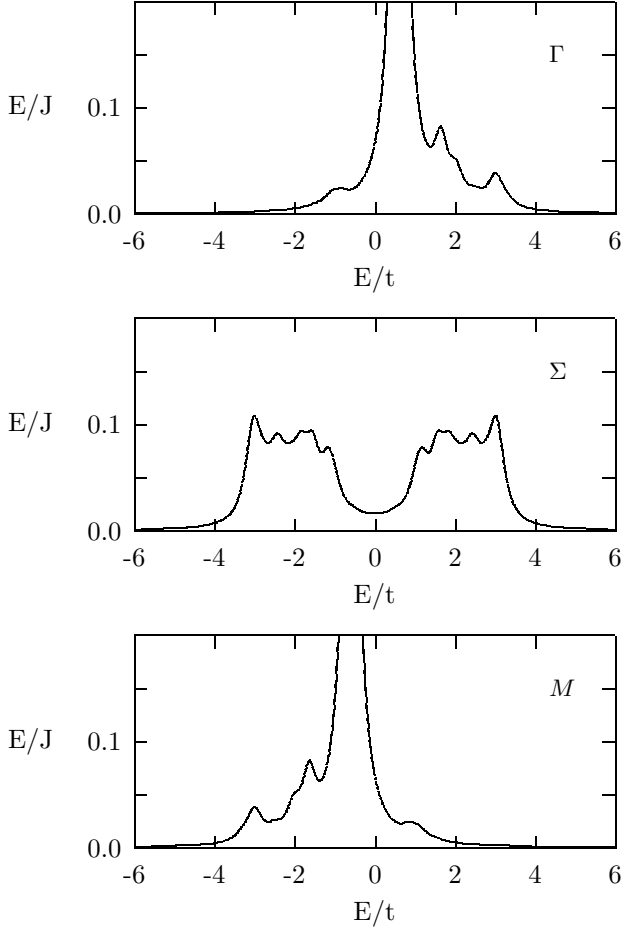


FIG. 5: $A_q(E) = -\text{Im}G_{q\sigma}(E)$ as defined by Eq. (12), computed by exact diagonalization on a 4×4 cluster by Dagotto⁶ for the case of $J/t = 0$.

later cannot be computed accurately but its integrated area can. Both sum rules are straight lines at low doping, the slope of which *does not depend on J* . This is the behavior of a doped semiconductor. From the usual expression

$$\int_0^\infty \sigma_{xx}(\omega) d\omega = \frac{\pi}{2} \frac{\hbar^2}{m} n, \quad (9)$$

we find a mass of

$$m = 0.77 \frac{\hbar^2}{tb^2}, \quad (10)$$

where b is the bond length. This compares favorably with the $1/\sqrt{2}$ in these same units obtained from the curvature of Eq. (5) near its minimum and the 0.54 obtained in 1-d from the Bethe solution. The fact that the “Drude” weight is always about half the total indicates that this particle is the carrier. The full sum rule

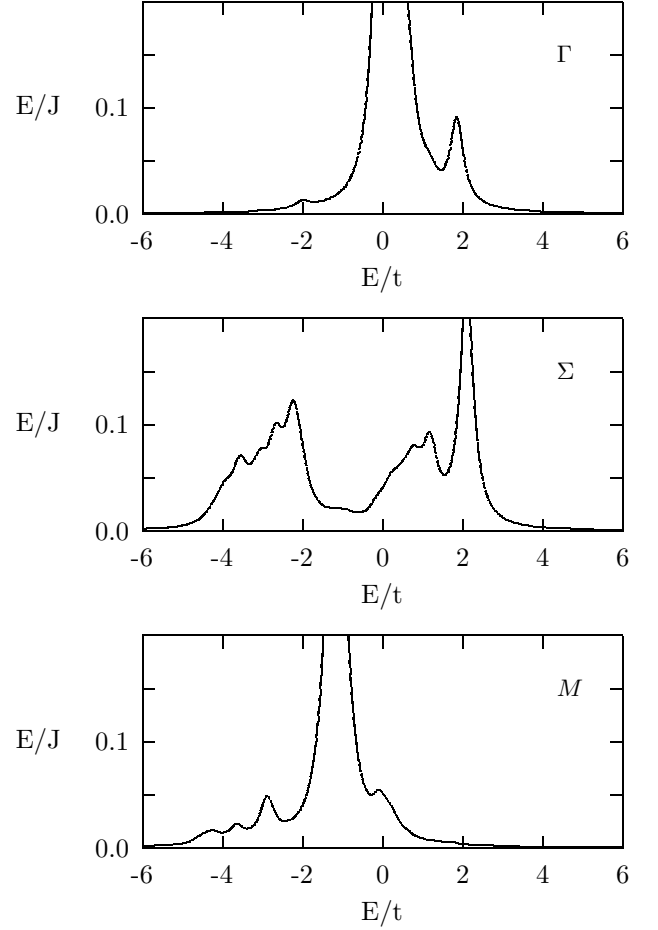


FIG. 6: Same as Fig. 5 except with $J/t = 0.2$

$$\langle T \rangle = -2.6 N t \delta \quad (11)$$

also agrees with Eq. (5) in equaling the $-\sqrt{8}t$ per hole associated with the holon band minimum. This number has no connection to the mass in general, and is thus an additional constraint on the band structure.

Further evidence for the existence of the holon may be found in the electron propagator in the limit of small J/t . Following the notation of Eq. (7), we define the electron propagator by

$$G_{q\sigma}(E) = \sum_{\alpha} \left\{ \frac{|\langle \alpha | c_{q\sigma}^{\dagger} | 0 \rangle|^2}{E - E_{\alpha} + E_0 + i\eta} + \frac{|\langle \alpha | c_{q\sigma} | 0 \rangle|^2}{E + E_{\alpha} - E_0 - i\eta} \right\} \quad (12)$$

where

$$c_{q\sigma} = \frac{1}{\sqrt{N}} \sum_j \exp(iq \cdot r_j) c_{j\sigma}. \quad (13)$$

In Figs. 5 and 6 I show the imaginary part of this function at half-filling calculated by the exact diagonalization

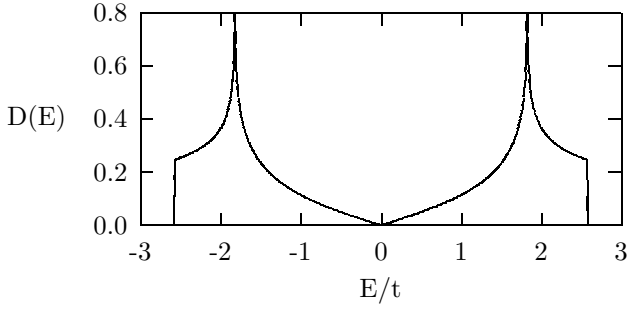


FIG. 7: Holon density of states defined by Eq. (14).

method for $J/t = 0.0$ and 0.2 by Dagotto⁶. In either case the spectrum is a broad continuum about $6t$ wide with a pronounced dip in the center and a weight that moves from low to high energy as the momentum is advanced from Γ to M . In the $J \rightarrow 0$ limit the broad continuum may be ascribed to the decay of the injected hole into spinon-holon pair in the limit that the spinon is very heavy, for then the spectrum should be the holon density of states

$$\mathcal{D}(E) = \frac{b^2}{2\pi^2} \sum_{\lambda} \int_{-\pi/b}^{\pi/b} \int_{-\pi/b}^{\pi/b} \delta(E - E_{q\lambda}^{\text{holon}}) dq_x dq_y \quad (14)$$

weighted by a decay matrix element. The density of states computed from Eq. (5) is plotted in Fig. 7. Any reasonable model will give the motion of the weight since

$$\langle 0 | c_{q\sigma}^\dagger c_{q\sigma} | 0 \rangle = \frac{1}{2} \quad (15)$$

$$\langle 0 | c_{q\sigma}^\dagger \mathcal{H} c_{q\sigma} | 0 \rangle = \langle 0 | \mathcal{H} | 0 \rangle$$

$$-2t \left[\frac{\langle \vec{S}_1 \cdot \vec{S}_2 \rangle}{3} - \frac{1}{4} \right] \left\{ \cos(q_x) + \cos(q_y) \right\} \quad (16)$$

at half-filling, where 1 and 2 denote near-neighbor sites.

The $J/t = 0.2$ curves also have a peak at low binding energy which is the quasiparticle of the magnetic insulator. In Fig. 8 I show the dispersion relation of this quasiparticle found numerically by a number of authors⁷. It has a deep minimum at Σ and an overall bandwidth W , the difference between the maximum and minimum of the dispersion relation, that *does not depend on t* . This width, measured in multiples of t , is plotted against J/t in Fig. 8⁸. From the slope of the line one obtains

$$W = 2.2J \quad , \quad (17)$$

or $1.6\sqrt{2}J$, which is the spinon bandwidth given by Eq. (4). The prefactor 1.6 in Eq. (4) has the physical significance of a magnetic stiffness. It causes the spinon

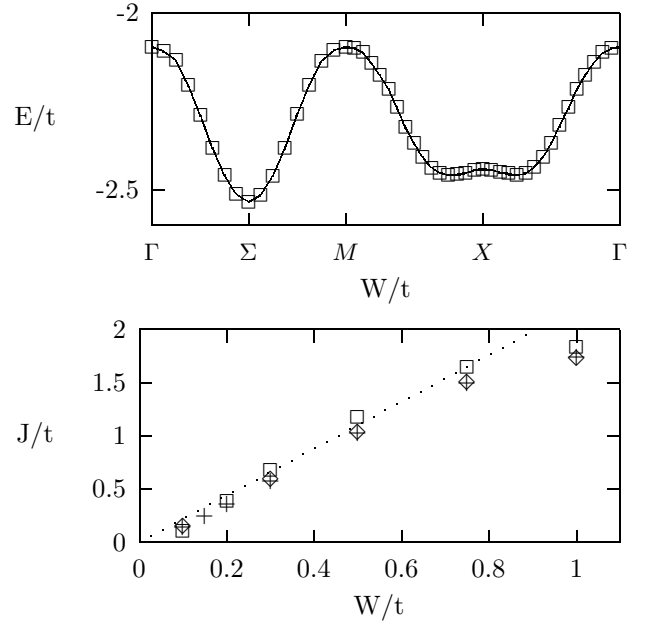


FIG. 8: Top: Quasiparticle dispersion relation calculated by Liu and Manousakis⁷ using spin-wave perturbation theory for the case of $J/t = 0.2$. Bottom: Quasiparticle bandwidth W/t calculated by Poilblanc⁸ using exact diagonalization on clusters of various sizes. The dotted line is a plot of Eq. (17).

velocity at Σ to be the spin-wave velocity of the ordered antiferromagnet⁹

$$v_s = 1.6 \frac{JB}{\hbar} \quad . \quad (18)$$

The quasiparticle peak is accompanied by scattering resonances. These cannot be seen in Fig. 4 because the sample is too small, but they may be seen clearly in Fig. 9, which is the spectral function at Σ for $J/t = 0.2$, calculated using spin wave perturbation theory⁷. The quasiparticle peak and the first two resonances are labeled by roman numerals. Their energies are plotted as a function of J/t in Fig. 9. The lines through the data points represent the formula

$$E_n/t = -3.28 + (J/t)^{2/3} \times \begin{bmatrix} 2.03; n=1 \\ 5.46; n=2 \\ 7.81; n=3 \end{bmatrix} \quad . \quad (19)$$

These energies are exactly the spectrum expected a light particle in orbit about a heavy one, provided the attractive force between the two is a *string*, i.e. $V(r) \sim |r|$. More precisely, the Hamiltonian

$$\mathcal{H} = -\frac{\hbar^2}{2m} \nabla^2 + 2.2 J \left| \frac{r}{b} \right| - 3.28t \quad , \quad (20)$$

where m is the mass derived by the conductivity sum rule and given explicitly by Eq. (10), has energy eigenvalues

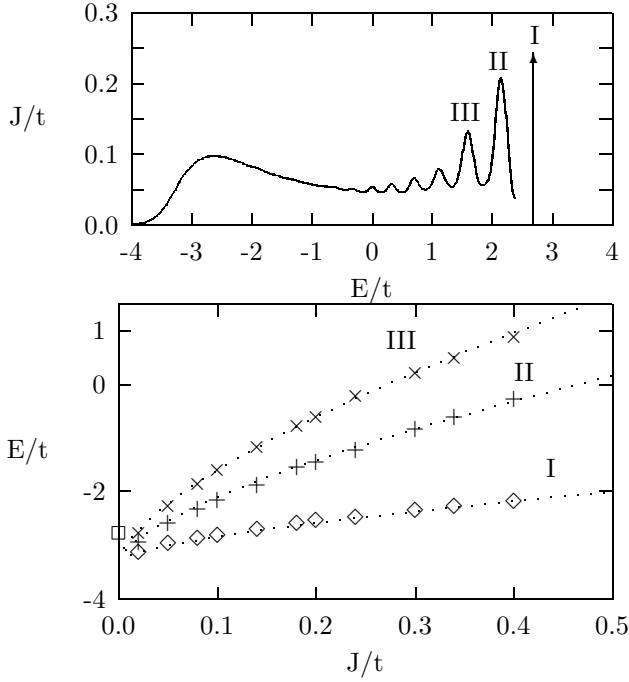


FIG. 9: Top: Spectral density at Σ calculated by spin wave perturbation theory by Liu and Manousakis⁷ for the case of $J/t = 0.1$ in the limit of large sample size. Bottom: Energies of quasiparticle (I) and first two string resonances (II and III) as a function of J/t . The dashed lines are plots of Eq. (19).

given by Eq. (19) except for substitution $(2.63, 5.54, 7.81) \rightarrow (2.03, 5.46, 7.81)$.

These facts have the following physical interpretation. The quasiparticle is a bound state of a spinon and the holon analogous to the hydrogen atom. Its band structure tracks that of the spinon because the spinon is “heavier” than the holon in the sense of having a narrower band. The optical sum rule, by contrast, is sensitive to the light particle, and thus measures the holon properties. The same thing is true in hydrogen, where the acceleration mass is dominated by the proton but the optical properties are dominated by the electron. The potential binding these particles together is a string at low doping, which means that they can never separate and do not exist as separate entities in this limit, but already at a doping of one hole in a 4×4 lattice, or $\delta = 1/16$, something occurs to allow the string to break and the holon to ionize off to become a free carrier.

The t-J Hamiltonian is formally equivalent to the Lagrangian^{3,4}

$$\mathcal{L} = \sum_j \left\{ \sum_{\sigma} f_{j\sigma}^{\dagger} \left[i\hbar \partial_t + \phi_j \right] f_{j\sigma} + b_j^{\dagger} \left[i\hbar \partial_t + \phi_j \right] b_j - \phi_j \right\} + \sum_{\langle j,k \rangle} \left\{ -\frac{J}{4} |\chi_{jk}|^2 \right.$$

$$\left. + \frac{J}{2} \chi_{jk}^* \left[\sum_{\sigma} f_{j\sigma}^{\dagger} f_{k\sigma} - \frac{2t}{J} b_j^{\dagger} b_k \right] - \frac{t^2}{J} b_j^{\dagger} b_k^{\dagger} b_k b_j \right\}, \quad (21)$$

where $f_{j\sigma}$ and b_j are fictitious fermion and boson operators on site j in terms of which the electron is written

$$c_{j\sigma} = f_{j\sigma} b_j^{\dagger}, \quad (22)$$

ϕ_j is a Lagrange multiplier which when integrated out forces the constraint

$$\sum_{\sigma} f_{j\sigma}^{\dagger} f_{j\sigma} + b_j^{\dagger} b_j = 1, \quad (23)$$

and χ_{jk} is a Hubbard-Stratonovich variable. This is a U(1) gauge theory to the extent that χ_{jk} may be approximated as having a fixed length, for then the phase functions as a vector potential along the bond $\langle j, k \rangle$, the scalar potential on site j being ϕ_j . This turns out to be a bad approximation for this particular Lagrangian, but we can imagine adiabatically transforming it into one for which $|\chi_{jk}|$ is fixed and for which a small Maxwell term

$$\mathcal{L}_{\text{Max}} = \frac{1}{g} \left\{ J \sum_{\langle j,k,\ell,m \rangle} \chi_{jk} \chi_{k\ell} \chi_{\ell m} \chi_{mj} + \frac{1}{J} \sum_{\langle j,k \rangle} |\hbar \partial_t \chi_{jk} + (\phi_j - \phi_k) \chi_{jk}|^2 \right\} \quad (24)$$

is added as a regulator. Then the classical saddle point has magnetic flux π per plaquette, the f- and b-particles become free particles with the relations of Eqs. (4) and (5), although with different coefficients, and we obtain conventional lattice QED with doubled fermions. The limit relevant to the low-doping numerical work is $g \rightarrow \infty$, which is strongly confining. Thus the string forces may be associated with confinement in strongly-coupled QED, the antiferromagnetic order in limit may be associated with the chiral symmetry breaking known to accompany confinement in this problem, and the spin wave, which is both the Goldstone of the broken symmetry and a bound pair of spinons, may be associated with the pion.

The correct appearance of a string force in the antiferromagnetically ordered phase suggests that the unbinding of the quasiparticle seen in Fig. 4 might indicate a first-order transition to a superconducting phase corresponding to the coulombic phase of the gauge theory. The magnetic order is known to disappear at about $\delta = 0.05$, which is consistent with deconfinement by $\delta = 1/16$. However it is only a suggestion, for the above Lagrangian is less accurate and more difficult to solve than the spin Hamiltonian from which it was derived,

and all the major ordering questions for the former are still unresolved. It should be viewed not as a computational tool but as means for understanding how the physics of the strong interactions might materialize in a quantum antiferromagnet without being postulated.

Acknowledgments

I wish to express special thanks to E. Dagotto for providing me his unpublished $J \rightarrow 0$ spectral functions and

to A. M. Tikofsky for numerous helpful discussions. This work was supported primarily by the NSF under grant No. DMR-9421888. Additional support was provided by the Center for Materials Research at Stanford University and by NASA Collaborative Agreement NCC 2-794.

* R. B. Laughlin: <http://large.stanford.edu>

¹ P.-A. Bares, G. Blatter, and M. Ogata, *Phys. Rev. B* **44**, 130 (1991).

² Z. Zou, J. L. Levy, and R. B. Laughlin, *Phys. Rev. B* **45**, 993 (1992); Z. Zou and R. B. Laughlin, *ibid.* **42**, 4073 (1990); R. B. Laughlin and Z. Zou, *ibid.* **41**, 664 (1989); X.-G. Wen, F. Wilczek, and A. Zee, *ibid.* **39**, 11413 (1989).

³ A. M. Tikofsky, R. B. Laughlin, and Z. Zou, *ibid.* **69**, 3670 (1989); R. B. Laughlin and A. M. Tikofsky, *Phys. Rev. B* **50**, 10165 (1994).

⁴ N. Nagaosa and P. A. Lee, *Phys. Rev. Lett.* **64**, 2450 (1990);

L. B. Ioffe and A. I. Larkin, *Phys. Rev. B* **39**, 8988 (1989).

⁵ E. Dagotto *et al.*, *Phys. Rev. B* **45**, 10741 (1992); A. Moreo and E. Dagotto, *ibid.* **42**, 4786 (1990); W. Stefan and P. Horsch, *ibid.*, 8736 (1990).

⁶ E. Dagotto, private communication.

⁷ Z. Liu and E. Manousakis, *Phys. Rev. B* **45**, 2425 (1992).

⁸ D. Poilblanc, H. J. Schulz, and T. Ziman, *Phys. Rev. B* **47**, 3268 (1993).

⁹ N. Trivedi and D. M. Ceperley, *Phys. Rev. B* **40**, 2737 (1989).